Journal of Applied Polymer Science

Self-assembling amphiphilic PEGylated block copolymers obtained through RAFT polymerization for drug-delivery applications

Claudio Colombo,[1] Simone Gatti,[2] Raffaele Ferrari,[3] Tommaso Casalini,[1] Danilo Cuccato,[1] Lavinia Morosi,[3] Massimo Zucchetti,[3] Davide Moscatelli[2]

[1]Institute for Chemical and Bioengineering, Department of Chemistry and Applied Biosciences, ETH Zürich, Vladimir-Prelog-Weg 1, 8093 Zürich, Switzerland

[2]Dipartimento di Chimica, Materiali ed Ingegneria Chimica, Politecnico Di Milano 20131, Milano

[3]IRCCS - Istituto di Ricerche Farmacologiche Mario Negri, Via La Masa 19, 20156, Milano, Italy

Correspondence to: D. Moscatelli (E-mail: davide.moscatelli@polimi.it)

ABSTRACT: In this work, ring-opening polymerization and reversible addition-fragmentation chain transfer polymerization (RAFT) have been employed for the production of block copolymers where the backbone is brushed with poly(ethylene glycol) (PEG) and polyester chains. Because of their amphiphilic properties, they are able to self-assemble in water, forming micelles. Molecular dynamics simulations have been accomplished to study the behavior of the copolymer single chain in water, and the self-assembly properties have been characterized and correlated to the copolymer structure in terms of critical micellar concentration and particle size. As a proof of their flexibility, these materials have been employed for the production of polymer–lipid hybrid nanoparticles with tunable dimensions (from 120 to 260 nm) adopted for the controlled release of anticancer compounds (paclitaxel and curcumin). © 2015 Wiley Periodicals, Inc. J. Appl. Polym. Sci. **2016**, *133*, 43084.

KEYWORDS: copolymers; drug-delivery systems; self-assembly

Received 25 June 2015; accepted 25 October 2015

DOI: 10.1002/app.43084

INTRODUCTION

Reversible addition-fragmentation chain transfer polymerization (RAFT) is a widely used and well-established methodology to produce block copolymers with controlled characteristics because of the large number of monomers it can be applied to, the mild reaction conditions, the absence of toxic metal catalysts, and the facility to perform postpolymerization functionalizations.[1,2] In addition, it allows the synthesis of different polymer structures such as block copolymers, which can find application as drug-delivery carriers due to the presence of both hydrophobic and hydrophilic brushes[3,4]: the former can be exploited to facilitate the entrapment of hydrophobic drugs, and the latter act as stabilizing agents, also decreasing the opsonization in the bloodstream.[5–7] Biodegradable polyesters are among the most commonly used materials for the production of polymeric nanoparticles (NPs) for drug-delivery applications because of their well-established biocompatibility and biodegradability; these materials often compose the hydrophobic core, and poly(ethylene glycol) (PEG) is often employed as a hydrophilic block.[8] In the literature, there are many reports on the synthesis and applications of linear polyester–PEG copolymers; the comb-like ones are far less common.[9–11] A comb-like PEGylated polyester-based material produced via RAFT would combine the benefit of comb-like polyesters (such as tunable degradation[12] and side-chain functionalizations[13]) and the advantages of the controlled RAFT process, like the possibility to obtain a selective chain-end functionalization and control the degree of polymerization, maintaining a very low polydispersity.[14,15]

In this work, a new class of self-assembling amphiphilic PEGylated block copolymers are synthetized by combining ring-opening polymerization (ROP) and RAFT polymerization to obtain polymers with a well-controlled comb-like structure. First, different PEGylated macro-CTAs (chain transfer agents) are obtained from RAFT polymerization of a PEGylated methacrylate, poly(ethylene glycol) methyl ether methacrylate (PEGMA); afterwards these compounds are used in the polymerization of a polycaprolactone (PCL)-based methacrylate macromonomer (HEMA-PCL) obtained via ROP.[16] The final product is a comb-like block copolymer with a controllable number of PEG and PCL chains [$(PEGMA)_m$-b-(HEMA-

Additional Supporting Information may be found in the online version of this article.

PCL)$_n$]. With the use of two types of controlled polymerization, it is possible to tune the length of the PCL chains and the length of the backbone; also, the polydispersity of the final polymer can be kept as low as 1.20, a result that can be very relevant in the biomedical field to produce monodisperse carriers with reproducible behavior.[17] The configuration of the single copolymer chain in water has been modeled with molecular dynamics (MD), confirming the influence of both hydrophilic and hydrophobic chains on the final polymer configuration.

These copolymers self-assemble in water to produce micelles with a critical micellar concentration (CMC) that is related to the structure of the starting material. Because of their characteristics, the copolymers have been used as stabilizing agents for the production of surfactant-free, hybrid polymer–lipid core–shell NPs using cholesterol as hydrophobic component through a conanoprecipitation process[11]; this particular class of carriers is considered very promising for biological applications because of their facile synthesis, low toxicity, and low production costs.[18] As a first evaluation of the application of these materials in this field, they have been loaded with anticancer compounds (paclitaxel and curcumin), and their release has been studied.

EXPERIMENTAL

Materials

The materials ε-caprolactone (CL, 97%), 2-hydroxyethyl methacrylate (HEMA, 97%), stannous octoate [Sn(Oct)$_2$, 98%], poly(ethylene glycol) methyl ether methacrylate (PEGMA, Mn 950 Da), 4,4′-azobis(4-cyanovaleric acid) (ACVA, 98%), 4-cyano-4-(phenylcarbonothioylthio)pentanoic acid (CTP, >97%), and cholesterol (96%) were purchased from Sigma-Aldrich (St. Louis, Missouri, United States) and used without further treatment except when specifically noted. All of the solvents used were of analytical-grade purity and were purchased from Sigma-Aldrich). Curcumin was supplied by Agros Organics (Geel, Belgium. Paclitaxel was supplied by Indena (Milan, Italy).

Block Copolymer Synthesis

Block copolymers are composed of two monomers: the hydrophilic commercially available PEGMA and the hydrophobic HEMA-PCL. The latter has been synthesized as reported in the literature.[16] Briefly, 30 mg of Sn(Oct)$_2$ were mixed with 3.8 g of HEMA in a 10-ml vial under magnetic stirring at room temperature until full dissolution of the Sn(Oct)$_2$. Meanwhile, 10 g of CL were heated up to 130°C in a stirred flask with the temperature controlled by an external oil bath. The HEMA/Sn(Oct)$_2$ solution was then added to the flask; the reaction was carried out for 2 h. At the end of the process, a macromonomer with an average of three units of caprolactone attached to a HEMA molecule is obtained because the molar ratio between caprolactone and HEMA was chosen to equal three. Characterization was carried out via ^{1}H-NMR analysis performed in $CDCl_3$; details can be found in the Supporting Information. Before use, both this monomer and PEGMA were dissolved in tetrahydrofuran and flowed through a basic alumina column to remove inhibitors.

The production of the block copolymers was performed through the synthesis of three different PEGMA-based macro-CTAs using a molar ratio between PEGMA and 4-cyano-4-(phenylcarbonothioylthio)pentanoic acid (CPPA) equal to 10, 20, and 40 in order to obtain (PEGMA)$_{10}$, (PEGMA)$_{20}$, and (PEGMA)$_{40}$ macro-CTA, respectively. As an example, for the latter case, PEGMA (3 g, 3.16 mmol), CPPA (22 mg, 0.0788 mmol), and 4,4′-azobis(4-cyanovaleric acid) (ACVA 7.4 mg, 0.0264 mmol) were dissolved in ethanol (7 mL), and the solution was purged by bubbling nitrogen for 20 minutes at room temperature and then heated to 60°C in an oil bath under nitrogen atmosphere and magnetic stirring. After 48 h the polymer was concentrated under vacuum, washed three times with diethyl ether to remove unreacted monomer, and characterized by gel permeation chromatography (GPC) and ^{1}H-NMR. For the GPC analysis, the apparatus (Agilent, 1100 series, Santa Clara, California, United States) was equipped with both ultraviolet and differential refractive index detectors. A precolumn and two PLgel 5 μm MIXED-C columns (Polymer Laboratories, Santa Clara, California, United States, length 300 mm and diameter 7.5 mm, measuring range 2000 to 2 $\times$ 10^6 Da) have been used. Chloroform was used as an eluent at a flow rate of 0.5 mL min^{-1} and a temperature of 30°C. Universal calibration was applied, based on polystyrene standards.

Every macro-CTA was then used to produce three different block copolymers with a molar ratio between HEMA-PCL and the macro-RAFT agent equal to 10, 20, and 40, respectively. For example, for the synthesis of (PEGMA)$_{40}$-b-(HEMA-PCL)$_{40}$, the (PEGMA)$_{40}$ macro-RAFT agent (1 g, 0.0263 mmol), the HEMA-PCL macromonomer (0.497 g, 1.05 mmol, molar ratio equal to 40), and ACVA (2.2 mg, 0.00789 mmol) were dissolved in ethanol (7 mL), and then the solution was purged by nitrogen and heated at 60°C for 24 h. The produced copolymer was then concentrated under vacuum, washed three times with diethyl ether, and characterized by GPC and ^{1}H-NMR. The final materials consist of a block copolymer with a controlled number of HEMA-PCL and PEGMA chains, hereinafter referred to as (PEGMA)$_m$-b-(HEMA-PCL)$_n$ where m and n can be equal to 10, 20, or 40.

Computational Methods

A model chain for the system was built adopting a syndiotactic configuration for the sequence of polymethacrylic diads composing the backbone. This polymer molecular model was then parameterized using the general AMBER force field (GAFF),[19] which proved to be suitable for the description of amphiphilic polymers in an aqueous environment.[20,21] Partial atomic charges for each monomer were determined starting from the electrostatic potentials computed through density functional theory calculations (B3LYP/6-31+g(d,p) level of theory)[22–24] in implicit water (modeled through IEF-PCM formalism)[25] at 300 K. Computations were performed by means of Gaussian 09 software.[26]

Atomic charges were then fitted adopting the RESP formalism,[27,28] assigning a global charge of zero to each monomer and imposing the same partial charge to chemically equivalent atoms.

Molecular dynamics simulations were carried out by means of the GROMACS package, version 4.5.5.[29] Electrostatic long-range interactions were treated through the particle mesh Ewald (PME) method,[30] using a cut-off value equal to 10 Å; the same

cutoff was adopted for Lennard-Jones interactions. The neighbor list was updated every 5 fs, and all covalent bonds involving hydrogen were restrained by means of the LINCS algorithm.[31]

The model chain was placed in a periodic box containing about 14,000 explicit TIP3P water molecules[32]; after a preliminary minimization, the temperature was raised to 300 K through 200 ps in the NVT ensemble, applying a small harmonic restraint to the solute in order to avoid wild fluctuations. Finally, all restraints were removed, and the polymer structure was equilibrated with a 200-ns simulation in the NPT ensemble at 300 K and atmospheric pressure. Temperature and pressure control was ensured through a velocity rescale thermostat and an anisotropic Berendsen barostat (London, United Kingdom), respectively.[33,34] Time steps equal to 1 fs along with the Leap-frog algorithm were adopted to compute molecular trajectories. Data were collected every 10 ps. All calculations were performed on the Brutus cluster of ETH Zürich, Switzerland.

Micelle Preparation and Characterization

Micelles were produced by dissolving selected amounts of the produced copolymer in 4 mL of deionized water. The solution was then left under sonication in an ultrasonic bath for 15 minutes. Micelles were characterized in terms of diameter and polydispersity via dynamic light-scattering measurements (DLS, Malvern Zetanano ZS, Worcestershire, United Kingdom) at 25°C. The particle size distribution of the samples was estimated adopting the cumulant method, or z-average diffusion coefficient, as defined by ISO (standard document ISO 13321:1996E) and reported in the literature.[35] In particular, the polydispersity index (PDI) of the NP size distribution was estimated from the first- and second-order cumulant of the light scattered intensity.[36] All OF the reported data are an average value of three measurements of the same sample.

The critical micellar concentration of the produced copolymers was determined with the same apparatus by evaluating the evolution of the scattered light intensity as a function of the copolymer concentration, as reported in the literature.[37] All of the solutions used for the study were prepared at least 48 h before the measurements. The reason for this long equilibration time is the slow self-assembly process of the block copolymers.[38]

Polymer–Lipid NP Synthesis and *In Vitro* Release

Polymer–lipid core–shell NPs were prepared through the conanoprecipitation method. A selected amount of cholesterol (from 1 to 10 mg) and $(PEGMA)_{40}$-b-$(HEMA\text{-}PCL)_{40}$ copolymer (from 1 to 10 mg) in a 1:1 weight ratio was dissolved in 1 ml of dimethylformamide. The organic phase was added to 3 mL of water with a syringe pump; the solution was kept under magnetic stirring (1200 rpm) for the whole addition (10 min). The NPs were then characterized using DLS, and a correlation between their size and the synthesis condition was established. The analyses were performed three times, and the reported data show the average of them; the standard deviations were always below 5%.

For *in vitro* release, curcumin-loaded NPs were prepared with the same procedure using 10 mg of $(PEGMA)_{40}$-b-$(HEMA\text{-}PCL)_{40}$ copolymer, 9.5 mg of cholesterol, and 0.5 mg of curcumin. After the synthesis, 0.5 mL of curcumin-loaded NP latex was put in 9.5 ml of phosphate-buffered saline (PBS)/dimethyl sulfoxide (DMSO) 9:1 vol/vol solution, where DMSO was used to increase the solubility of curcumin in the aqueous phase. The solution was put in a closed 20-mL vial and left under gentle magnetic stirring at 37°C in an incubator. At selected times, small aliquots of the solution (0.1 ml) were withdrawn and replaced with fresh medium. The supernatant of the withdrawn samples was recovered using Vivaspin 500 filters (Sartorius Stedim, Göttingen, Germany). Each aliquot was added to the Vivaspin and was centrifuged at 4000 rpm for 15 min. To ensure the complete recovery of the supernatant, the following procedure was applied two times: 0.1 ml of PBS/DMSO solution was added to the Vivaspin filter and the system was centrifuged at 4000 rpm for 15 min. From the evaluation of the absorbance of the supernatant, it was possible to determine the amount of curcumin released.

Paclitaxel (PTX)-loaded NPs were prepared using the same procedure but using PTX instead of curcumin. For this case, 3 mL of PTX-loaded NPs at a concentration of 15 μg/mL were put in a dialysis membrane and dialyzed against 200 ml of PBS. The amount of drug in the NP solution and in the supernatant was determined by high performance liquid chromatography (HPLC) analysis with UV detection (Waters Associates, Milford, MA, model 2487 Variable Wavelength Detector, wavelength: 230 nm). Briefly, 0.1 mL of the NP solution was spiked with 5 µg of internal standard IDN5390 and extracted with 0.5 ml of CH_3CN. After a vortex for 10 s, samples were centrifuged at 13,000 rpm for 10 min. The organic phase was separated and dried under nitrogen, and the residues were dissolved with 250 μl of the mobile phase. Then 50 µL of the reconstituted sample was injected into the HPLC system. The apparatus is equipped with a Symmetry C18 column (Agilent, Santa Clara, California, USA; 5 μm, 4.6 × 150 mm); the mobile phase is composed of 50% ammonium acetate buffer (0.01*M*, pH 5), 40% acetonitrile, and 10% methanol with a flux rate of 1.3 ml/min and 30-min run time. The evaluation of the loading efficiency was determined by evaluating the drug within the supernatant as for the curcumin. For both compounds, the loading efficiency was calculated as follows:

$$\%\ \text{loading efficiency} = \left(1 - \frac{\text{drug recovered in the supernatant (t=0)}}{\text{total drug added to the system}}\right) \cdot 100 \quad (1)$$

RESULTS AND DISCUSSION

Block Copolymer Synthesis

The synthesis of the $(PEGMA)_m$-b-$(HEMA\text{-}PCL)_n$ block copolymers was carried out in three steps by combining the ROP of ε-caprolactone and RAFT polymerization. The idea is to create a biocompatible block copolymer containing a biodegradable lipophilic block with a good control over the molecular weight of both the hydrophilic block and the backbone. The overall process and the structure of the final block copolymers are reported in Scheme 1.

The ^{1}H-NMR analysis of the HEMA-PCL macromonomer is discussed in the Supporting Information. The results obtained for the production of the PEGMA-based macro-CTAs and the

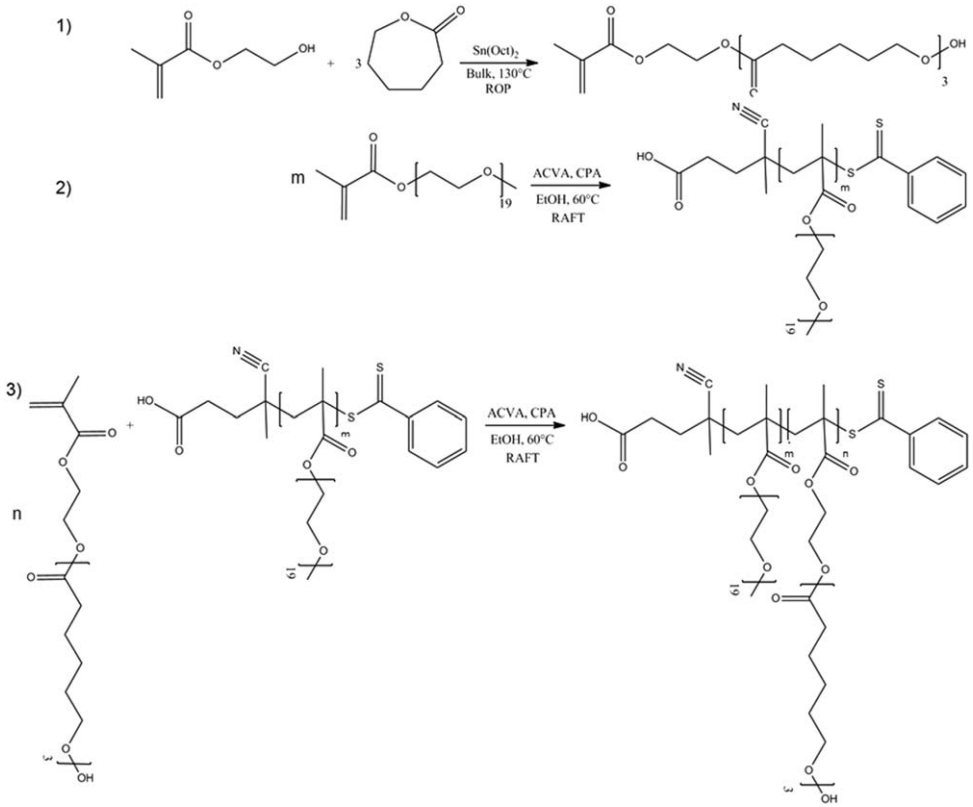

Scheme 1. Reaction scheme for the production of block copolymers. The first step is the ROP of caprolactone initiated by HEMA, followed by the production of the PEGylated macro-CTA. Finally, the HEMA-PCL monomer is copolymerized using the PEGylated macro-CTA to produce the block copoymer.

block copolymers produced are summarized in Table I and Figure 1. Typically, for the production of block copolymers with RAFT polymerization, a good choice of the order of blocking is important because the first block produced should be a good macro-CTA for the second monomer, and it is not always possible to find a good solvent for both the macro-CTA and the second monomer when an arbitrary choice of the order of blocking is made. However, in this case the macromonomers used are both methacrylates and thus possess similar reactivity. Ethanol is found to be a good solvent for both the macromonomers and polymers, and despite its mild nucleophilicity, which can eventually lead to the degradation of the RAFT end group,[39]

Table I. Characterization of Macro-CTA and Block Copolymers Produced

Sample	M_n Theory[a] [Da]	M_n GPC[b] [Da]	PD [-]	Conversion (χ)[c] [-]
$(PEGMA)_{10}$	7109	11777	1.09	0.683
$(PEGMA)_{20}$	14981	19712	1.17	0.735
$(PEGMA)_{40}$	36040	35581	1.18	0.895
$(PEGMA)_{10}$-b-$(HEMA\text{-}PCL)_{10}$	11839	15757	1.16	0.829
$(PEGMA)_{10}$-b-$(HEMA\text{-}PCL)_{20}$	16569	18475	1.17	0.815
$(PEGMA)_{10}$-b-$(HEMA\text{-}PCL)_{40}$	26029	25005	1.15	0.795
$(PEGMA)_{20}$-b-$(HEMA\text{-}PCL)_{10}$	19711	23283	1.14	0.832
$(PEGMA)_{20}$-b-$(HEMA\text{-}PCL)_{20}$	24441	28453	1.21	0.911
$(PEGMA)_{20}$-b-$(HEMA\text{-}PCL)_{40}$	33901	32970	1.22	0.878
$(PEGMA)_{40}$-b-$(HEMA\text{-}PCL)_{10}$	40770	38046	1.29	0.885
$(PEGMA)_{40}$-b-$(HEMA\text{-}PCL)_{20}$	45500	42933	1.30	0.869
$(PEGMA)_{40}$-b-$(HEMA\text{-}PCL)_{40}$	54960	47356	1.20	0.928

[a] Obtained by the equation $M_n = \frac{[M]_0 X}{[CTA]_0} M_{n,mon} + M_{n,CTA}$.
[b] In $CHCl_3$ with Poly(Styrene) calibration.
[c] Conversion was determined by comparing the area of the UV signal of the monomer at t_0 and at t_{final}.

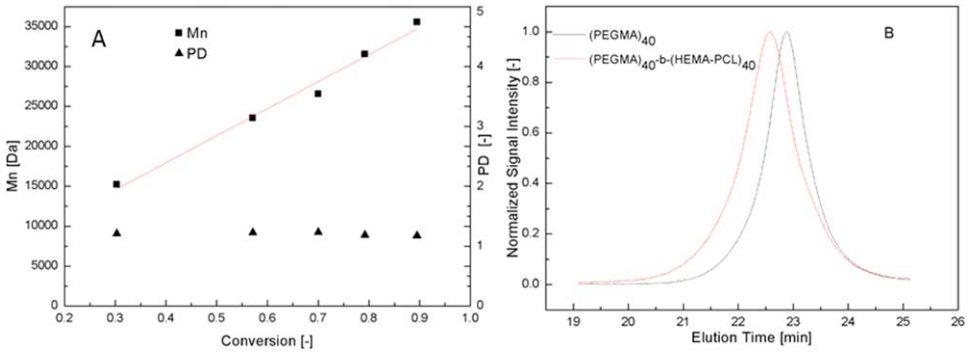

Figure 1. (A) Molecular weight and polydispersity as a function of conversion for the production of the $(PEGMA)_{40}$ macro-CTA. (B) Shift in the elution peak from the $(PEGMA)_{40}$ macro-CTA (black line) to the final $(PEGMA)_{40}$-b-$(HEMA\text{-}PCL)_{40}$ copolymer. [Color figure can be viewed in the online issue, which is available at wileyonlinelibrary.com.]

the good agreement between the theoretical and experimental polymer properties found for this system show that this side reaction is negligible.

To prove that a good control over the molecular weight is possible in a wide range for this system, different CTAs and different block copolymers were synthesized. The results of the synthesis are summarized in Table I, which shows that both good correspondence between the theoretical molecular weights and the ones obtained via GPC (using universal calibration) and low values of polydispersity (PD) were always found for both homopolymers and block copolymers. The change in the molecular

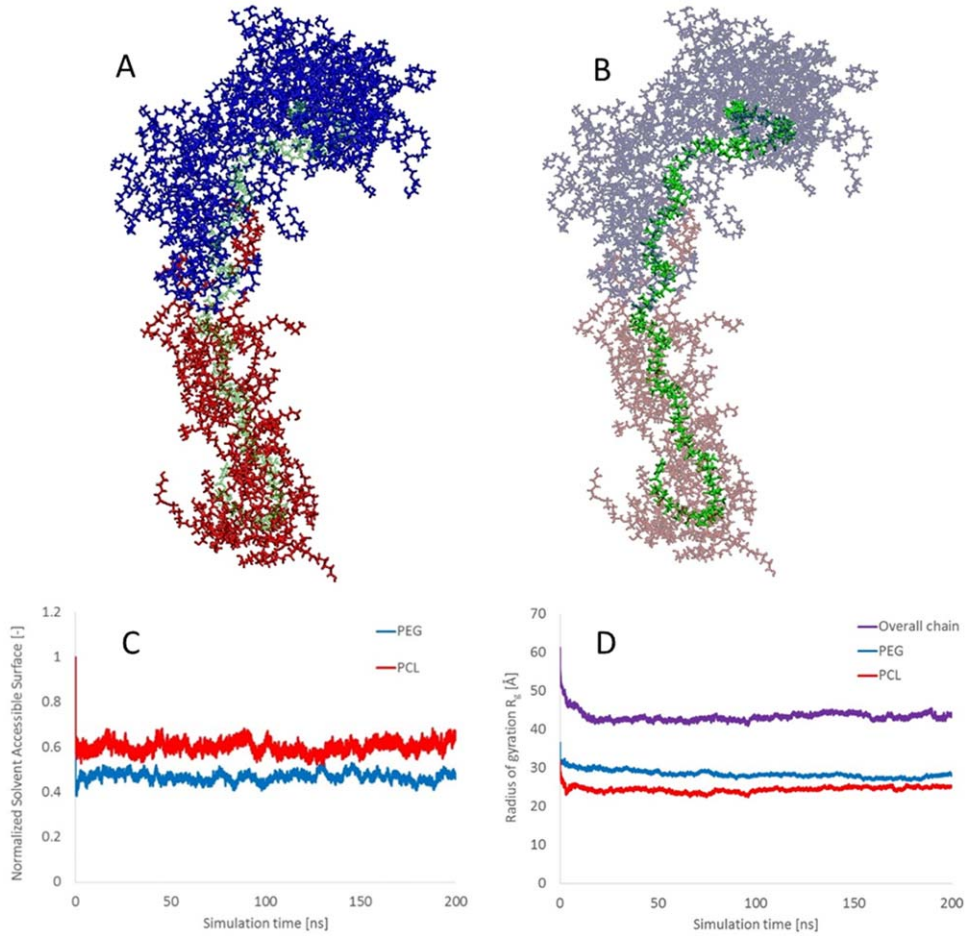

Figure 2. Equilibrated structure of $(PEGMA)_{40}$-b-$(HEMA\text{-}PCL)_{40}$ block copolymer in water environment at 300 K from 200 ns molecular dynamics simulation; explicit water molecules are omitted for the sake of clarity. PCL chains are red (A), PEG chains are blue (A), and the backbone is green (B). Also shown are the normalized solvent-accessible surface (C) and the radius of gyration (D) as a function of simulation time. [Color figure can be viewed in the online issue, which is available at wileyonlinelibrary.com.]

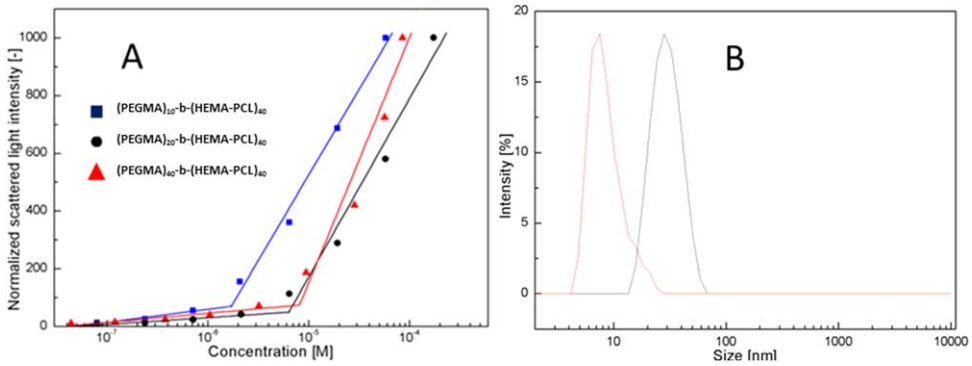

Figure 3. (A) CMC determination via DLS for selected macromonomers in water. (B) DLS analysis of the $(PEGMA)_{40}$-b-$(HEMA\text{-}PCL)_{40}$ micelles (black line) and size distribution obtained under the CMC for the same material (red line). [Color figure can be viewed in the online issue, which is available at wileyonlinelibrary.com.]

weight and PD as a function of the monomer conversion is shown in Figure 1 for the case of $(PEGMA)_{40}$ macro-CTA.

A linear dependence of M_n (number-average molecular weight) with conversion can be seen in Figure 1(A) with the typical hybrid behavior that was already observed for this kind of PEG-based methacrylate.[40] Nevertheless, as is shown in Figure 1(B) for the case of $(PEGMA)_{40}$-b-$(HEMA\text{-}PCL)_{40}$, the polymer produced has a monomodal and narrow molecular-weight distribution with a polydispersity equal to 1.18. This compound can be effectively used as a macro-CTA to produce a block copolymer with a size exclusion chromatography (SEC) trace shifted to lower elution time without changing shape and keeping a low polydispersity.

Molecular Dynamics

MD simulations have been performed in order to characterize the structure of the $(PEGMA)_{40}$-b-$(HEMA\text{-}PCL)_{40}$ block copolymer in water at room temperature. A representative structure, obtained after a simulated time of 200 ns, is reported in Figure 2.

Both PEG and PCL chains experience a fast folding process, as indicated by the sudden decrease in the value of the solvent-accessible surface (SAS) at the beginning of the simulation [Figure 2(C)]. In particular, the SAS values have been normalized with respect to the corresponding values that PEG and PCL would exhibit if they assume the full stretched conformation [Figure S5(D), reported in the Supporting Information], which was employed as input for the MD simulation. The SAS values of PEG and PCL decrease by about 50% and 60%, respectively, compared to the corresponding initial values. As expected, the radius of gyration R_g decreases to about 4.4 nm as well, due to the folding process [Figure 2(D)]. This value is in good agreement with the hydrodynamic radius of a single chain, equal to 3.9 nm, obtained through DLS analysis under CMC conditions *(vide infra)*, confirming the structural insights obtained through MD. The polymer backbone does not undergo a full folding process, but rather keeps an elongated structure, while the chain-end fragments coil up in order to promote the mutual favorable interactions between the side chains.

Micelle Characterization

For the production of micelles and NPs aimed at intravenous drug delivery, the $(PEGMA)_{40}$-b-$(HEMA\text{-}PCL)_{40}$ was chosen because of its high PEG content, which should decrease opsonization and risk of thrombogenicity.[41] Results concerning the micellization are reported in Figure 3.

From Figure 3(A) it is possible to see the nonlinear relationship between concentration and scattered light intensity: the CMC value that can be derived for the $(PEGMA)_{40}$-b-$(HEMA\text{-}PCL)_{40}$ macromonomer is 8.3×10^{-6} M. For comparison, the CMC for the $(PEGMA)_{20}$-b-$(HEMA\text{-}PCL)_{40}$ and $(PEGMA)_{10}$-b-$(HEMA\text{-}PCL)_{40}$ are found at 6.2×10^{-6} M and 1.7×10^{-6} M, respectively, thus confirming that the CMC value decreases with the increase of the hydrophobic content in the copolymers. In Figure 3(B) the particle size distribution of the micelles produced by the self-assembly of $(PEGMA)_{40}$-b-$(HEMA\text{-}PCL)_{40}$ is reported (size = 27.4 nm, PDI = 0.101). The size distribution for the same material under the CMC is centered at a radius of 3.9 nm; this value corresponds to the hydrodynamic radius of the single chain in water, and it is very close to the radius of gyration found by molecular dynamics simulations (4.4 nm).

Polymer–Lipid NP Synthesis and Release

Due to the presence of both lipophilic and hydrophilic chains, the produced materials have been used in a conanoprecipitation process as stabilizing agents for composite polymer–lipid carriers able to deliver different compounds and with dimensions suitable to exploit the enhanced permeability and retention (EPR) effect in solid tumors. The influence of the solid content in the organic phase on the final NP characteristics has been studied, and a correlation was found, as reported in Figure 4.

As shown in Figure 4(A), as the solid concentration is increased, the NPs become bigger, ranging from 120 nm to 260 nm. In addition, the measured PDI values are low, less than 0.15, thus confirming the nanoparticle monodispersity. This behavior is similar to the classic nanoprecipitation processes, where a higher solid concentration enhances particle growth with respect to particle nucleation.[42] In Figure 4(B) the ability of the produced carriers to load hydrophobic antitumor agents, curcumin and PTX, and their subsequent release *in vitro* are shown. For both compounds, a high loading efficiency (91% and 95%,

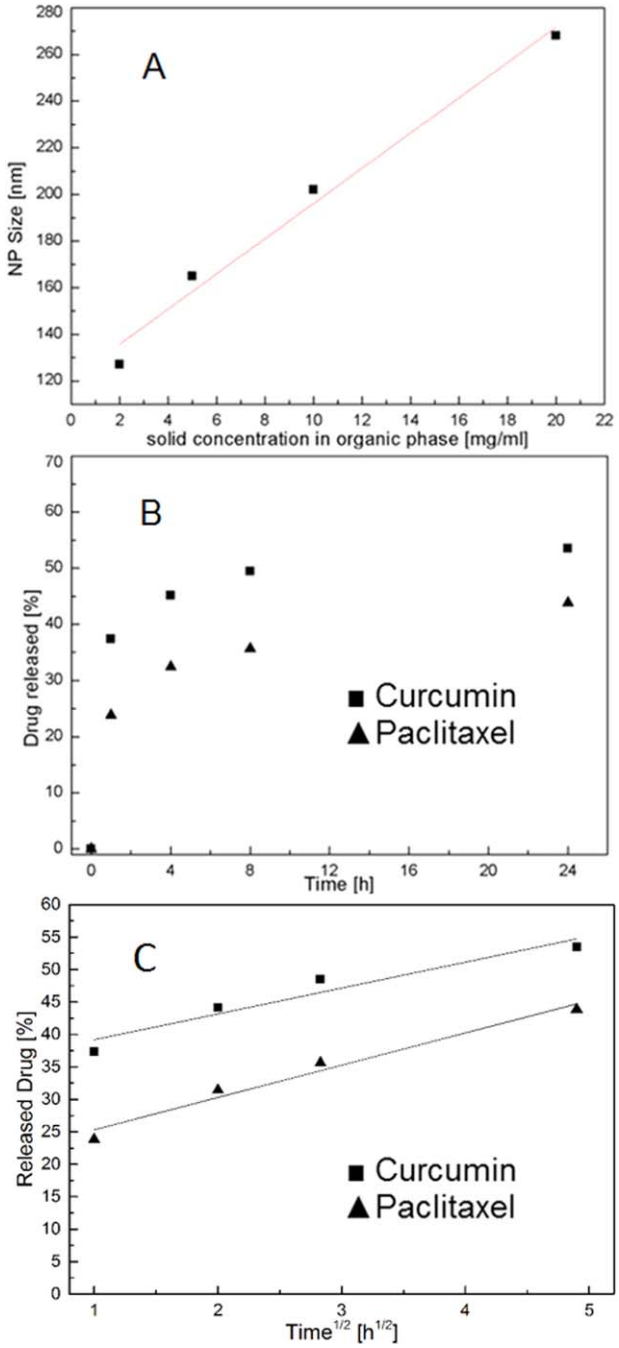

Figure 4. (A) Correlation between solid concentration and NP size. (B) Release profiles of curcumin (squares) and PTX (triangles). (C) Release profiles plotted against square root of time. [Color figure can be viewed in the online issue, which is available at wileyonlinelibrary.com.]

respectively) can be obtained. For the *in vitro* release, we choose to finish the sampling at 24 h because this is compatible with the typical half-life of polymeric NPs in the bloodstream. The release profile of PTX appears to be steeper than the one of curcumin, despite the relatively higher water solubility of PTX.[43] This is due to the different fluid used for the release of curcumin from the NPs (PBS:DMSO 9:1 instead of PBS), which increases its affinity to the liquid phase. As expected, the release profile is similar for both drugs, showing an initial burst release in the first hour, likely due to the dissolution of the drug that was adsorbed on the nanoparticle surface, followed by a slower and continuous release phase, which may be attributed to the diffusion of the drug localized in the core of the nanoparticles, confirming that it is possible to achieve sustained release from these NPs. In Figure 4(C) the release profiles of both drugs are plotted against the square root of time, and a linear correlation can be found. This proves that the drug is being released via a pure Fickian mechanism due to diffusion.[44]

CONCLUSIONS

In this work, a combination of RAFT and ROP have been employed to synthesize PEGylated caprolactone-based block copolymers for drug-delivery applications. Because of the peculiar synthetic pathway employed, it was possible to obtain materials with low polydisperisity (PD = 1.14–1.30) and controllable characteristics. The ability of the produced materials to self-assemble in water to produce micelles was studied. Moreover, molecular dynamics simulations have been employed to obtain insights concerning the structure of the block copolymer in an aqueous environment. A selected copolymer was chosen as a stabilizing agent for the production of hybrid lipid–polymer NPs, whose dimensions can be tuned from 120 to 260 nm by changing the synthesis conditions. The possibility to load hydrophobic drugs into these NPs and their subsequent release *in vitro* was also evaluated, confirming that the produced materials represent a flexible tool for drug-delivery applications.

ACKNOWLEDGMENTS

We acknowledge support from AIRC Special Program Molecular Clinical Oncology "5 per mille."

AUTHOR CONTRIBUTIONS

C. Colombo and S. Gatti contributed equally in the experimental work and in writing the major part of the article. T. Casalini and D. Cuccato worked on the molecular dynamic simulation part. L. Morosi and M. Zucchetti worked on the release of paclitaxel from the nanoparticles. R. Ferrari and D. Moscatelli contributed in the design of the article and revising it critically. All of the authors gave their final approval on the version to be submitted.

REFERENCES

1. Chong, Y. K.; Le, T. P. T.; Moad, G.; Rizzardo, E.; Thang, S. H. *Macromolecules* **1999**, *32*, 2071.
2. Quemener, D.; Davis, T. P.; Barner-Kowollik, C.; Stenzel, M. H. *Chem. Commun.* **2006**, *48*, 5051.
3. Pang, X.; Zhao, L.; Feng, C.; Wu, R.; Ma, H.; Lin, Z. *Polym. Chem.* **2013**, *4*, 2025.
4. Li, Q.; Xiao, X.; Zhang, X.; Zhang, W. *Polymer* **2013**, *54*, 3230.
5. Yuan, W.; Yuan, J.; Zhou, L.; Wu, S.; Hong, X. *Polymer* **2010**, *51*, 2540.

6. Ferrari, R.; Yu, Y.; Lattuada, M.; Storti, G.; Morbidelli, M.; Moscatelli, D. *Macromol. Chem. Phys.* **2012**, *213*, 2012.
7. Sheng, Y.; Yuan, Y.; Liu, C.; Tao, X.; Shan, X.; Xu, F. *J. Mater. Sci. Mater. Med.* **2009**, *20*, 1881.
8. Kamaly, N.; Xiao, Z.; Valencia, P. M.; Radovic-Moreno, A. F.; Farokhzad, O. C. *Chem. Soc. Rev.* **2012**, *41*, 2971.
9. Gref, R.; Lück, M.; Quellec, P.; Marchand, M.; Dellacherie, E.; Harnisch, S.; Blunk, T.; Müller, R. H. *Colloids Surf. B* **2000**, *18*, 301.
10. Cheng, J.; Teply, B. A.; Sherifi, I.; Sung, J.; Luther, G.; Gu, F. X.; Levy-Nissenbaum, E.; Radovic-Moreno, A. F.; Langer, R.; Farokhzad, O. C. *Biomaterials* **2007**, *28*, 869.
11. Layre, A.; Couvreur, P.; Chacun, H.; Richard, J.; Passirani, C.; Requier, D.; Benoit, J. P.; Gref, R. *J. Controlled Release* **2006**, *111*, 271.
12. Colombo, C.; Dragoni, L.; Gatti, S.; Pesce, R. M.; Rooney, T. R.; Mavroudakis, E.; Ferrari, R.; Moscatelli, D. *Ind. Eng. Chem. Res.* **2014**, *53*, 9128.
13. Du, J.-Z.; Du, X.-J.; Mao, C.-Q.; Wang, J. *J. Am. Chem. Soc.* **2011**, *133*, 17560.
14. York, A. W.; Huang, F.; McCormick, C. L. *Biomacromolecules* **2010**, *11*, 505.
15. Luo, K.; Yang, J.; Kopečková, P.; Kopeček, J. I. *Macromolecules* **2011**, *44*, 2481.
16. Ferrari, R.; Yu, Y. C.; Morbidelli, M.; Hutchinson, R. A.; Moscatelli, D. *Macromolecules* **2011**, *44*, 9205.
17. Gaspar, R.; Duncan, R. *Adv. Drug Delivery Rev.* **2009**, *61*, 1220.
18. He, Z. Y.; Chu, B. Y.; Wei, X. W.; Li, J.; Carl, K. E.; Song, X. R.; He, G.; Xie, Y. M.; Wei, Y. Q.; Qian, Z. Y. *Int. J. Pharm.* **2014**, *469*, 168.
19. Wang, J. M.; Wolf, R. M.; Caldwell, J. W.; Kollman, P. A.; Case, D. A. *J. Comput. Chem.* **2004**, *25*, 1157.
20. Kasimova, A. O.; Pavan, G. M.; Danani, A.; Mondon, K.; Cristiani, A.; Scapozza, L.; Gurny, R.; Moller, M. *J. Phys. Chem. B* **2012**, *116*, 4338.
21. Torres, D. A.; Garzoni, M.; Subrahmanyam, A. V.; Pavan, G. M.; Thayumanavan, S. *J. Am. Chem. Soc.* **2014**, *136*, 5385.
22. Becke, A. D. *J. Chem. Phys.* **1993**, *98*, 5648.
23. Lee, C. T.; Yang, W. T.; Parr, R. G. *Phys. Rev. B* **1988**, *37*, 785.
24. Ditchfield, R.; Hehre, W. J.; Pople, J. A. *J. Chem. Phys.* **1971**, *54*, 724.
25. Mennucci, B.; Cances, E.; Tomasi, J. *J. Phys. Chem. B* **1997**, *101*, 10506.
26. Frisch, M. J.; Trucks, G. W.; Schlegel, H. B.; Scuseria, G. E.; Robb, M. A.; Cheeseman, J. R.; Scalmani, G.; Barone, V.; Mennucci, B.; Petersson, G. A.; Nakatsuji, H.; Caricato, M.; Li, X.; Hratchian, H. P.; Izmaylov, A. F.; Bloino, J.; Zheng, G.; Sonnenberg, J. L.; Hada, M.; Ehara, M.; Toyota, K.; Fukuda, R.; Hasegawa, J.; Ishida, M.; Nakajima, T.; Honda, Y.; Kitao, O.; Nakai, H.; Vreven, T.; Montgomery, J., J. A.; Peralta, J. E.; Ogliaro, F.; Bearpark, M.; Heyd, J. J.; Brothers, E.; Kudin, K. N.; Staroverov, V. N.; Kobayashi, R.; Normand, J.; Raghavachari, K.; Rendell, A.; Burant, J. C.; Iyengar, S. S.; Tomasi, J.; Cossi, M.; Rega, N.; Millam, N. J.; Klene, M.; Knox, J. E.; Cross, J. B.; Bakken, V.; Adamo, C.; Jaramillo, J.; Gomperts, R.; Stratmann, R. E.; Yazyev, O.; Austin, A. J.; Cammi, R.; Pomelli, C.; Ochterski, J. W.; Martin, R. L.; Morokuma, K.; Zakrzewski, V. G.; Voth, G. A.; Salvador, P.; Dannenberg, J. J.; Dapprich, S.; Daniels, A. D.; Farkas, Ö.; Foresman, J. B.; Ortiz, J. V.; Cioslowski, J.; Fox, D. J. Gaussian 09; Gaussian, Inc.: Wallingford, CT, **2009**.
27. Bayly, C. I.; Cieplak, P.; Cornell, W. D.; Kollman, P. A. *J. Phys. Chem.-US* **1993**, *97*, 10269.
28. Cornell, W. D.; Cieplak, P.; Bayly, C. I.; Kollman, P. A. *J. Am. Chem. Soc.* **1993**, *115*, 9620.
29. Hess, B.; Kutzner, C.; van der Spoel, D.; Lindahl, E. *J. Chem. Theory Comput.* **2008**, *4*, 435.
30. Essmann, U.; Perera, L.; Berkowitz, M. L.; Darden, T.; Lee, H.; Pedersen, L. G. *J. Chem. Phys.* **1995**, *103*, 8577.
31. Hess, B. *J. Chem. Theory Comput.* **2008**, *4*, 116.
32. Jorgensen, W. L.; Chandrasekhar, J.; Madura, J. D.; Impey, R. W.; Klein, M. L. *J. Chem. Phys.* **1983**, *79*, 926.
33. Bussi, G.; Donadio, D.; Parrinello, M. *J. Chem. Phys.* **2007**, *126*, 014101.
34. Berendsen, H. J. C.; Postma, J. P. M.; Vangunsteren, W. F.; Dinola, A.; Haak, J. R. *J. Chem. Phys.* **1984**, *81*, 3684.
35. Vega, J. R.; Gugliotta, L. M.; Gonzalez, V. D.; Meira, G. R. *J. Colloid Interface Sci.* **2003**, *261*, 74.
36. Perevyazko, I.; Vollrath, A.; Hornig, S.; Pavlov, G. M. Schubert, U. S. *J. Polym. Sci. A: Polym. Chem.* **2010**, 48, 3924.
37. Davis, B. M.; Richens, J. L.; O'Shea, P. *Biophys. J.* **2011**, *101*, 245.
38. Lamprou, A.; Xie, D.; Storti, G.; Wu, H. *Colloid Polym. Sci.* 2014, *292*, 677.
39. Willcock, H.; O'Reilly, R. K. *Polym. Chem.* **2010**, *1*, 149.
40. Pietsch, C.; Fijten, M. W.; Lambermont-Thijs, H. M.; Hoogenboom, R.; Schubert, U. S. *J. Polym. Sci. A: Polym. Chem.* **2009**, *47*, 2811.
41. Lai, B. F. L.; Creagh, A. L.; Janzen, J.; Haynes, C. A.; Brooks, D. E.; Kizhakkedathu, J. N. *Biomaterials* **2010**, *31*, 6710.
42. Lince, F.; Marchisio, D. L.; Barresi, A. A. *J. Colloid Interface Sci.* **2008**, *322*, 505.
43. Letchford, K.; Liggins, R.; Burt, H. *J. Pharm. Sci.* **2008**, *97*, 1179.
44. Ritger, P. L.; Peppas, N. A. *Journal of Controlled Release*, **1987**, *5*, 23.